Surface and flexoelectric polarization in a nematic liquid crystal directly measured by a pyroelectric technique

L. M. Blinov,[1,*] M. I. Barnik,[1] M. Ozaki,[2] N. M. Shtykov,[1] and K. Yoshino[2]

[1]*Institute of Crystallography, Russian Academy of Sciences, 117333 Leninsky prospekt 59, Moscow, Russia*

[2]*Department of Electronic Engineering, Graduate School of Engineering, Osaka University, 2-1 Yamada-Oka, Suita, Osaka 565-0871, Japan*

An alternative, pyroelectric effect based technique was developed for the direct measurement of the surface polarization in homogeneously and homeotropically oriented nematic cells as well as for the measurement of the flexoelectric polarization in hybrid aligned nematic cells. The pyroelectric response was measured with a modulated beam of a diode laser, absorbed by a dye incorporated in a standard liquid crystal 4-pentyl-4'-cyanobiphenyl. The dye provided a gradient of the temperature increment along the cell normal, which allowed for the separation of pyroelectric contributions from both the opposite surfaces and the bulk. The signs and absolute magnitude of the polarizations mentioned have been found over the entire temperature range of the nematic phase.

PACS number(s): 77.84.Nh, 64.70.Md, 77.70.+a

I. INTRODUCTION

Nematic liquid crystals are uniaxial media with a preferable direction of molecular axes **n** called ''the director.'' The states of the director **n** and -**n** are indistinguishable (no polar axis) and the nematic phase does not show spontaneous polarization. A typical nematic cell consists of two glasses (in the x,y plane) with a gap between them (along the z axis) filled with a liquid crystal. At the interface with a glass (or indium-tin oxide electrode), the mirror symmetry along the z axis is broken and the macroscopic polarization may arise perpendicular to the interface [1]. The microscopic reasons for this surface polarization P_s may be different: preferable asymmetric attachment of dipolar molecules to the interface; ion adsorption or the spatial dependence of the nematic-order parameter S; so-called order-electric polarization [2],

$$\mathbf{P}_0 = r_1(\mathbf{n} \cdot \text{grad}S)\mathbf{n} + r_2 \, \text{grad}S. \tag{1}$$

The latter is especially important for the nematic phase where grad$S$ at an interface with a substrate might be very large (r_1 and r_2 are ordoelectric coefficients). The surface polarization arises in a very thin (of the order of 10 nm) surface layer for any (planar, homeotropic, or tilted) alignment of a liquid crystal. In a symmetric cell, say, planar or homeotropic, $\mathbf{P}_s$ vectors at the two interfaces face opposite directions, providing zero total polarization.

A macroscopic polarization may also be induced in the bulk of a nematic liquid crystal by a bend or splay distortion of the director field. A commonly used term for that polarization is a flexoelectric one, and its general form satisfying symmetry requirements [3] is

$$\mathbf{P}_f = e_1\mathbf{n} \, \text{div} \, \mathbf{n} - e_3(\mathbf{n} \times \text{curl} \, \mathbf{n}), \tag{2}$$

which consists of two terms with correspondent flexoelectric coefficients e_1 and e_3 related to the splay and bend distor-

tions. From the microscopic point of view, the dense packing of dipolar banana- or pear-shaped molecules in a bent or splayed structure inevitably creates a dipole moment in a unit space. In the case of nonpolar molecules, the flexoelectric effect originates from a gradient of quadrupole moment density [4].

The flexoelectric polarization arises in nematic cells with a hybrid alignment, planar at one interface and homeotropic at the opposite interface, Fig. 1. In this case, **n** $=(\sin\vartheta, 0, \cos\vartheta)$ with $\vartheta_0 = \pi/2$ at $z=0$ and $\vartheta_d=0$ at $z=d$, where $\vartheta(z)$ is an angle the director forms with the normal (z) to the plates and d is layer thickness. In this particular case, we have a very simple form from Eq. (2) for the z component of the flexoelectric polarization:

$$P_f = \langle P_f^z \rangle = \frac{1}{d}\int_0^d P_f^z \, dz$$

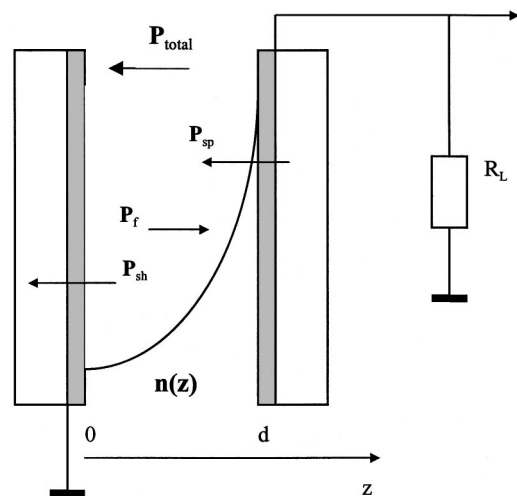$$= \frac{e_1 + e_3}{4d}(\cos 2\vartheta_0 - \cos 2\vartheta_d) = \frac{e_1 + e_3}{2d}. \tag{3}$$

FIG. 1. Distribution of the director **n**(z) and three components of the total polarization studied in a hybrid nematic cell.

---

*Author to whom correspondence should be addressed. Fax: +7-095-1351011. Electronic address: lev@glasnet.ru

Generally speaking, in a hybrid cell we have three contributions to the total z component of polarization, namely, one from the bulk (P_f) and two from the planar and homeotropic surfaces, P_{sp} and P_{sh}:

$$P_{\text{total}} = P_f + P_{sp} + P_{sh}. \quad (4)$$

The three components are shown in Fig. 1; the sign of each contribution will be discussed later on.

Despite the fact that the concept of the surface and flexoelectric polarization has been discussed for many years, the quantitative data are very scarce. The surface polarization manifests itself in experiments on the optical second-harmonic generation from the solid–liquid-crystal interface [5,6], but its sign and the absolute magnitude are controversial and the temperature dependence is not known. Estimations of the surface polarization (about 100 pC/m) have been made from observations of surface instabilities [7]. The flexoelectric polarization seems to influence electro-optical phenomena, defect formation, structural instabilities, etc. [8]. Its measurements are a real challenge because the polarization is always screened by free charge carriers and there is no simple way to switch it and observe repolarization currents, as is routinely done in the case of ferroelectric liquid crystals. What is usually measured is the inverse effect: when an electric field is applied, an alignment of a liquid crystal becomes distorted. Since the pioneer work of Schmidt *et al.* [9] different techniques have been suggested to measure flexoelectric coefficients [10–16]; but, in fact, the accuracy of those measurements is influenced by a number of parameters involved (dielectric and optical anisotropy, elastic moduli, field inhomogeneity, etc.) and additional problems arise with the determination of a sign of the effect. Moreover, with few exceptions, only the difference (e_1-e_3) is measured (for collection of data see [16]).

The aim of the present paper is to show how the temperature dependence of the surface and flexoelectric polarization of a nematic liquid crystal can be measured directly in typical planar, homeotropic, and hybrid aligned nematic sandwich cells. The experiments have been carried out using a specially developed, steady-state ac pyroelectric technique on a standard compound 4-pentyl-4′-cyanobiphenyl (5CB) for which, at present, no reliable experimental data on temperature dependencies of the flexoelectric and surface polarization are available.

The paper is organized as follows. First, we describe our experimental technique. Next, we show the results of the measurements of the pyroelectric response in uniform planar and homeotropic cells. Then we discuss a more complicated case of a hybrid cell in which all three polarizations are essential, Fig. 1, and describe a procedure for the separation of each contribution (up to this point the experiments have been carried out on a dye-doped 5CB using a steady state technique). After this we find the absolute sign and magnitude of the total polarization of a hybrid cell using data obtained with a pulse laser technique and pyroelectric measurements of a ferroelectric liquid crystal (FLC) with well known spontaneous polarization. Finally, we present and discuss the absolute data on the temperature dependencies of the surface polarizations P_{sp} and P_{sh} (coming from the nematic ordering) and the flexoelectric one, P_f.

II. EXPERIMENT

A. Principle

Our main idea is to use the pyroelectric response of a nematic cell to a spatially dependent temperature increment in order to separate the contributions to the macroscopic polarization coming from both the surfaces and the bulk. In crystallography, by definition, the pyroelectric coefficient is $\gamma_0 = dP_0/dT$, where P_0 is the spontaneous polarization of a crystal and T is the temperature. In a more general case, instead of the spontaneous polarization we may consider any macroscopic polarization P^*, not necessarily spontaneous, and introduce a macroscopic pyroelectric coefficient

$$\gamma = \frac{dP^*}{dT}. \quad (5)$$

If we are interested only in effects coming from the nematic (N) ordering and not from the isotropic (I) background, we can calculate the temperature dependence of P^* in the nematic phase by integrating the pyroelectric coefficient starting from a certain temperature T_i above the N-I transition:

$$P^*(T) = \int_{T_i}^{T} \gamma(T) dT. \quad (6)$$

The main advantage of the pyroelectric technique is that it may be possible to find the sign and the absolute value of the macroscopic polarization *without application of an external field*. Therefore any effects related to the screening of the field are not involved. This technique has been widely used for measurements of the spontaneous and field-induced (electroclinic) polarization in ferroelectric liquid crystals (see, e.g., [17])

In order to measure $\gamma(T)$, we have to change the temperature of a sample by a small amount ΔT. Using light absorption one can create a desirable profile of $\Delta T(z)$ ranging from one that is almost uniform (weak light absorption) to one that is almost stepwise (strong absorption). The former is better for measurements of bulk polarization (e.g., P_f); the latter allows for the probing polarization of surface layers (P_{sp} and P_{sh}).

B. Samples

In our experiments, we used 10–11 μm thick planar (PP), homeotropic (HH), and hybrid (HP) cells prepared from tin dioxide covered glass plates. The thickness was determined from capacitance measurements of sealed empty cells. The electrodes were covered with unidirectionally rubbed polyimide for planar orientation and a surfactant (chromium distearyl chloride) for homeotropic orientation. The cells were filled with either pure 4-pentyl-4′-cyanobiphenyl 5CB (for calibration) or 5CB doped with 1 wt. % *t*-butylphthalocyanine of vanadyl (PcVO); see inset to Fig. 2. PcVO was necessary to provide a desirable profile of light absorption of the laser diode used in pyroelectric measurements. The absorption spectrum of a HH cell filled with 1% PcVO doped 5CB is shown in Fig. 2. The absorption maximum (810 nm) is very close to the laser line (820 nm); therefore, almost complete absorption is provided by only 1% of the dye in 10 μm thick cells of any type. Moreover, due to a disk shape of the PcVO the anisotropy of absorption is small
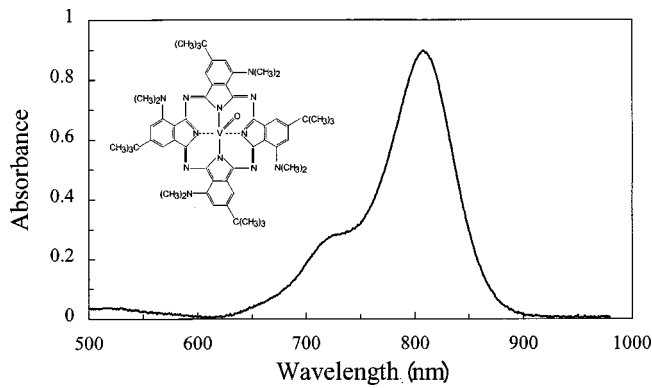
FIG. 2. The absorption spectrum of a HH (homeotropic) cell filled with 1% PcVO doped 5 CB. Inset: a chemical formula of *t*-butyl-phthalocyanine of vanadyl (PcVO).

(dichroic ratio is less than 1.5, even for PP cells at room temperature). The latter is very important for our experiments based on comparison of the absorption dependent pyroelectric response for different cells.

The 1 wt. % concentration of the dye reduced the T_{NI} transition point by only 1–2 °C. We have investigated several samples of each type and the results were quite reproducible. Table I shows the thickness (d), area (Ar), dielectric permittivity (ϵ at $f = 1$ kHz), and absorbance (optical density D) in the isotropic phase at $T = 40$ °C ($D = \log_{10} I_0 / I$ where I_0 and I are incident and transmitted light intensities at $\lambda = 820$ nm) of only those three samples that are discussed below. The parameters are consistent with those expected for high quality HH, PP, and HP cells. The cells were placed in a thermal jacket supplied with a Pt thermometer, which allowed for automatic measurements of temperature with an accuracy to ±0.1 K.

C. ac pyroelectric measurements

The scheme of the pyroelectric setup used for measurements of the pyroelectric response of our cells on an arbitrary scale is shown in Fig. 3. Basically, it is the so-called Chynoweth dynamic technique. A cell in the thermal jacket is installed under a microscope and irradiated through an ocular hole of the microscope by a beam of a diode laser providing 30 mW power in the continuous regime at $\lambda = 820$ nm. The laser beam is modulated with square-wave pulses from a function generator. As a rule, we used a modulation frequency of 127.5 Hz, although some experiments have been done with higher frequencies. The transmitted intensity was measured by a large area photodiode installed
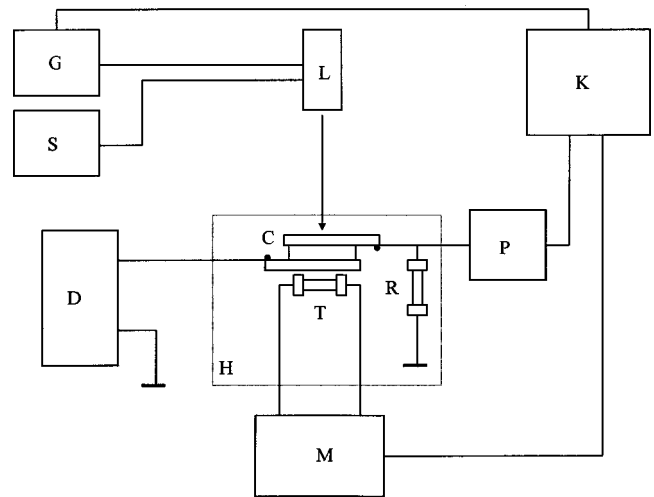
TABLE I. Parameters of the cells studied.

Cell	Material	d, μm	Ar, cm^2	ε	D
HH	5 CB (1% PcVO)	10.0	0.260	17.9	0.75
PP	5 CB (1% PcVO)	10.3	0.254	7.2	0.77
HP	5 CB (1% PcVO)	11.0	0.270	13.2	0.91
FLC	ZhK 1005	11.0	0.250	47.0	0.84
	(1% PcVO)	47.0[a]			0.84[b]

[a]Without bias.
[b]In Sm-C^*.

FIG. 3. Scheme of the ac pyroelectric setup: C, cell; L, laser diode; G, function generator; R, load resistor; P, selective preamplifier; K, PC computer; H, thermostat; T, Pt thermometer; M, multimeter; D, dc source; S, voltage source for the laser diode.

under the thermal jacket and shunted by a 500 ohm resistor (to operate in the linear regime). The radiation, absorbed by the dye, causes liquid crystal temperature modulation. Due to temperature dependent polarization, a pyroelectric current flows through the external circuit at the frequency of modulation. The response is taken in the form of the voltage U_p across the load resistor R shunted by the cell impedance and the input of a selective preamplifier tuned to frequency f. In order to reduce the influence of the cell impedance on comparative measurements of different cells we have used rather low input resistance of the preamplifier (1 Mohm parallel to $R = 5$ MOhm). The pyroelectric signal from the preamplifier was measured by a ''virtual lock-in amplifier based on a multimedia card of an IBM computer'' [18] synchronized by the output of the photodiode measuring the optical transmission. In this way, we could measure temperature, the optical transmission, and the amplitude and phase of the pyroelectric response simultaneously during the same temperature scan. All the measurements were carried out automatically with PHYSLAB software developed by Palto (for more details see [18]).

The absolute calibration of the amplitude of the pyroelectric response necessary for determination of the pyroelectric coefficient has been done with the help of a ferroelectric liquid crystal (FLC) with known spontaneous polarization. To this effect, the FLC mixture ZhK1005 (manufactured by NIOPIK, Moscow) was doped with the same amount (1%) of PcVO, and a ferroelectric cell of the same thickness (Table I) was prepared. The temperature dependence of the spontaneous polarization P_0 (and therefore pyrocoefficient dP_0/dT) of the doped mixture was measured by a standard repolarization current technique and the pyroelectric coefficients of nematic cells found by comparison.

The main drawback of the ac pyroelectric technique is that it is difficult to find an absolute sign of the polarization measured because of phase shifts in the input circuit. Therefore for the absolute measurements of the sign of the pyroelectric coefficient we used the technique developed earlier [19]. A 10-μm HH cell filled with pure 5CB was irradiated
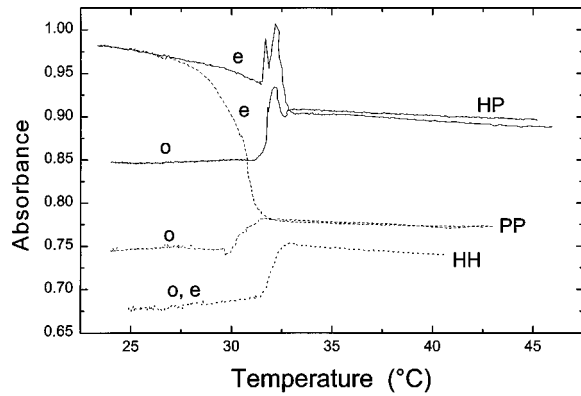
FIG. 4. Temperature dependencies of the absorbance of homeotropic (dotted lines), planar (dashed lines), and hybrid (solid lines) cells for e and o polarizations of laser light ($\lambda = 820$ nm).

by pulses of a Nd^{3+}-YAG laser (Spectron Laser Systems) operating in the continuous wave regime (wavelength 1.064 μm, pulse duration $t_p = 100 \, \mu$s, frequency 5 Hz, average incident power 40 mW, spot with diameter 5 mm completely covering the cell area $3.5 \times 5 \, mm^2$). The light was partially absorbed (about 38%) by both ITO electrodes, providing a temperature increment in the bulk of about 0.05 K. The pulse pyroelectric response was measured by a digital oscilloscope ($R = 800$ kohm) and the sign of the response was read out directly from the screen.

III. ABSORBANCE AND PYROELECTRIC RESPONSE

A. Absorbance

Here we are going to discuss experimental data on the pyroelectric response of the three cells (HH, PP, and HP, Table I) to a modulated beam of the laser diode. Figure 4 shows the temperature dependence of absorbance for the three cells at the laser wavelength 820 nm (e and o polarized). The cooling rate was the same for all the curves—0.1 K/min averaged over the whole scan, with 0.02 K/min in the vicinity of the transition. A general behavior of the curves is consistent with the good quality of homeotropic, planar, and hybrid cells. The difference in absorbance in the isotropic phase is accounted for by a difference in the thickness of the cells (about 10 μm for HH and PP cells and about 11 μm for the HP cell).

The structure of the absorption curves in the vicinity of the N-I transition is determined by the type of texture that appears at the transition. The optical features first appear for the HH cell (in the form of ''crosses''), then for the HP one (mixed), and finally for the PP cell (in the form of ''beans''). It may be understood if one remembers that we deal with the first order phase transition where all peculiarities are related to the formation of nuclei of the nematic phase. The amount and structure of the latter depend on a surface alignment.

For comparison of pyroelectric data for different cells, we should have a similar profile of the absorption. Fortunately, due to a plane shape of phthalocyanine dye the dichroism is small (in Fig. 4 the total ordinate scale is $D = 0.68 - 1.0$ and even less, $D_o = 0.68 - 0.92$, for the o polarization of laser light). Therefore to provide a similar absorption profile in all cases, we always used an incident light with an electric vector perpendicular to the director (o polarization for the PP

and HP cells). In addition, when calculating the pyroelectric coefficients and corresponding surface and flexoelectric polarizations, we made corrections for *absorbed light power* $A = 1 - T_{opt}$ by normalizing the pyroelectric response to $A = 0.83$ over the whole temperature range (T_{opt} is optical transmission).

B. Homeotropic cell

The pyroelectric response $U_p^m \sin(\omega t + \varphi)$ has different phase angle φ for different cells. Therefore to make a correct comparison of their response we measured and processed the $X = U_p^m \sin \omega t$ and $Y = U_p^m \cos \omega t$ components separately. The temperature dependencies of the X and Y components of the pyroelectric signal taken from the HH cell are shown on the top of Fig. 5. The curves were recorded on slow cooling of the cell. The X component corresponds to the phase of absorbed laser intensity, that is, to temperature increment $\Delta T_m \sin \omega t$; the Y component is shifted by $\pi/2$ and corresponds to the phase of time derivative $d\Delta T_m/dt$ of the increment. For bulk pyroelectrics, the Y component is usually dominating because the pyroelectric current is proportional to $dP_0/dt = \gamma_0 dT/dt$. For our HH cell, the total signal is coming from the two interface layers, and each of them contributes proportionally to their own temperature increment but with opposite sign. Therefore the total signal is proportional to the factor $(1 - \xi)$, where $\xi = \Delta T_r/\Delta T_f$ is the ratio of the temperature increments at the rear (ΔT_r) and front (ΔT_f) boundaries (ξ is to be found later on, in Sec. IV). The additional phase shift (nonzero X component) appears due to the fact that the main source of the response is the surface layer at the illuminated (front) electrode and the ac pyroelectric current is transmitted to the amplifier through the capacity of the bulk of the material.

The pyroelectric signal is already observed in the isotropic phase. It is accounted for by the temperature dependence of a background surface polarization independent of the nematic-order parameter. We cannot calculate this polarization due to a lack of the initial point for integrating the pyrocoefficient. Fortunately, the background signal is small and almost independent of temperature, and further on we shall subtract it (separately for X and Y components).

At the I-N phase transition, a considerable growth of the pyroelectric signal occurs with a typical maximum observed, e.g., in ferroelectric liquid crystals [17]. It means that below the phase transition, a new (nematic) contribution to the surface polarization appears with a rather large temperature slope. This polarization will be found by integrating the pyroelectric coefficient as soon as the increment ratio ξ becomes known and the absolute calibration of the pyroelectric response is done (see below).

C. Planar cell

The temperature dependencies of the X and Y components of the pyroelectric signal measured for the PP cell are shown in Fig. 5 (bottom). The regime of the measurements and a general temperature behavior of the components are the same as in the previous case. As in the case of absorbance, Fig. 4, the apparent temperature of the transition (say, the maximum of the Y component) is shifted down by 1.5 K for the PP cell with respect to that for the HH cell.
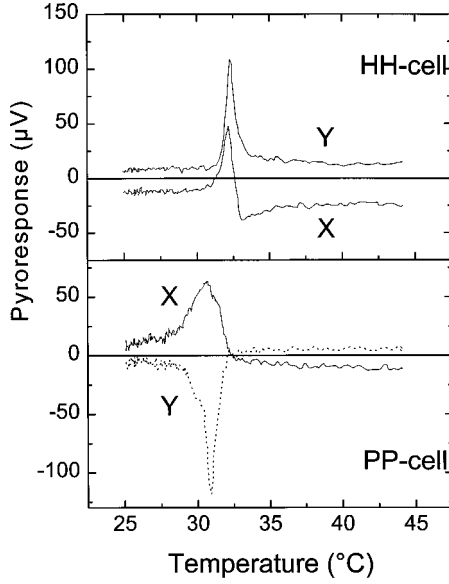
FIG. 5. Temperature dependencies of the X and Y components of the pyroelectric response (at the amplifier input) of two cells measured on cooling with average rate 0.1 K/min. Illumination from the front surface; the rear electrode is grounded. Top: Homeotropic (HH); bottom: planar (PP) cell, o polarization.

The signs of the X and Y components in the isotropic phase are the same as in the previous case. Most probably, the background polarization of the planar and homeotropic interface has the same direction and the same temperature behavior (less probable but not excluded is the situation when those signs are opposite and the temperature dependence is reversed for the two cases). Note, however, that, *in the nematic phase well below the phase transition*, the signs of both X and Y components are opposite to those for the HH cell. We may conclude immediately that the direction of the ''nematic'' surface polarization *is opposite for the planar and homeotropic orientation* (at least, for the type of surface treatment we used). This conclusion is very important for understanding the properties of hybrid cells since, in the latter, the vectors of the surface polarization *at the opposite electrodes* (planar and homeotropic) look *in the same direction* (do not compensate for each other) and contribute considerably to the total polarization.

D. Hybrid cell

The measurements of the pyroresponse of the HP cell have been done in two regimes upon illumination of the cell
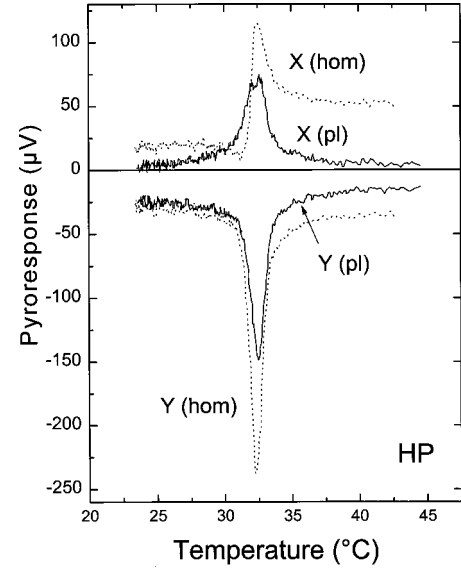

FIG. 6. Temperature dependencies of the X and Y components of the pyroelectric response of hybrid cell HP measured on cooling with average rate 0.1 K/min. Incident beam is o polarized. Homeotropic electrode is grounded; see Fig. 1. Solid lines, illumination from the planar side; dotted lines, illumination from the homeotropic side.

by an o-polarized light beam from the planar and homeotropic interface. This gives us an opportunity to calculate the contributions of both the planar and homeotropic interfaces and the bulk of the cell to the total response. Figure 6 shows the temperature dependencies of the X and Y components of the pyroelectric response upon illumination from the planar (solid lines) and homeotropic (dots) sides (the homeotropic electrode is grounded). Despite the fact that the general features of the two regimes are similar, note a substantial increase (decrease) of the response in the isotropic phase when the homeotropic (planar) side is illuminated. The reason is related to either constructive or destructive interference of the planar and homeotropic interface contributions to the total signal, which enables us to find the increment ratio ξ.

E. Ratio of the temperature increments

This ratio can easily be found in the isotropic phase because, in this case, the flexoelectric polarization vanishes and only pyroelectric signals from the two opposite interfaces (no matter of what nature) contribute to the total response. It is sufficient to solve the following set of equations the same way for the X and Y components of the response:

$$H(1-\xi)=a_{XY} \quad \text{(homeotropic cell)}, \tag{7a}$$

$$P(1-\xi)=b_{XY} \quad \text{(planar cell)}, \tag{7b}$$

$$P-\xi H=c_{XY} \quad \text{(hybrid cell, illuminated from the planar side)}, \tag{7c}$$

$$\xi P-H=d_{XY} \quad \text{(hybrid cell, illuminated from the homeotropic side)}. \tag{7d}$$

Here H and P (with subscripts X,Y omitted for simplicity) are unknown parameters, the pyroresponse of solely homeotropic and solely planar interface in the isotropic phase (note that signs at H and P are the same in Eqs. (7c) and (7d) because although the direction of the light beam is changing, we have not changed the electric circuit; the homeotropic electrode remained grounded); a, b, c, and d with corresponding subscripts are X and Y components of the total pyroresponse measured for different cells at the same temperature in the isotropic phase. In principle, we can find two values of ξ (ξ_X and ξ_Y) that are not necessarily equal. Moreover, Eqs. (7c) and (7d) are not independent, and, in fact, we can find four different values of ξ [two pairs of ξ_X and ξ_Y using either Eq. (7c) or Eq. (7d)]. The experimental parameters a, b, c, and d for X and Y components measured specially at the same temperature 43 °C are presented in Table II.

From the data of Table II and Eqs. (7a)–(7d) we have calculated the following values of the increment ratio: $\xi_{pX} = 0.6$, $\xi_{pY} = 0.48$, $\xi_{hX} = 0.59$, and $\xi_{hY} = 0.42$ (subscripts p,h indicate an illuminated interface; X,Y are related to the components of the response). It is seen that the direction of illumination plays a minor role ($\xi_{pX} \approx \xi_{hX}$, and ξ_{pY} is close to ξ_{hY}); however, the difference between the X and Y components is higher. The reason for the latter is not clear. Anyhow, the discrepancy is not high and we may take an average value of $\xi = 0.52 \pm 0.1$.

We have also made numerical calculations of a distribution of the temperature increment over the cell thickness z (at frequency ω of light modulation),

$$\Delta T(\omega, z, t) = \Delta T(\omega, z)\exp(i\omega t), \qquad (8)$$

from the thermal conductivity equation. We assumed that thermal energy is delivered by light absorbed in a liquid crystal and dissipated due to thermal diffusion in the liquid crystal and two limiting glass plates:

$$\frac{d^2 \Delta T}{dz^2} - \frac{i\omega}{\alpha_L}\Delta T = -\frac{I_0 \beta}{2 k_L}\exp(-\beta z), \qquad (9)$$

$$\frac{d^2 \Delta T}{dz^2} - \frac{i\omega}{\alpha_G}\Delta T = 0. \qquad (10)$$

Here k is the thermal conductivity of liquid crystal ($k_L = 0.16$ W/mK taken for 4-methoxy-benzylidene-4'-butylaniline (MBBA) from [8]) and glass ($k_G = 1.4$ W/mK taken from [20]); $\alpha = k/c\rho$ are the thermal diffusion coefficients for liquid crystal ($\alpha_L = 1.2 \times 10^{-7}$ m²/s) and glass ($\alpha_G = 8 \times 10^{-7}$ m²/s), (ρ and c are the density and specific

TABLE II. Experimental values of the pyroresponse (in μV) at 43 °C used for the calculation of temperature increment ratio ξ.

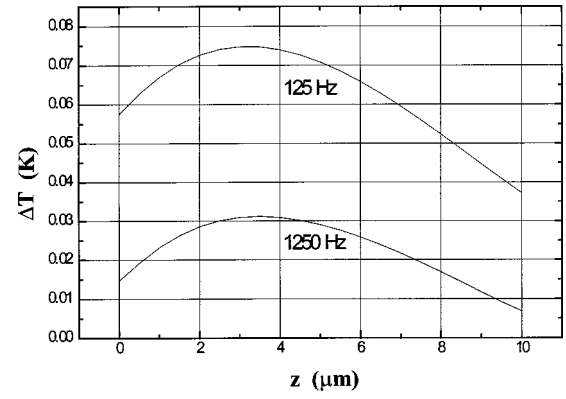| Parameter	X component	Y component
a	-26	$+11.8$
b	-14.2	$+3.2$
c	$+3.2$	-6.3
d	$+43$	-17.7

FIG. 7. Calculated light-induced increase in temperature (increment ΔT) as a function of distance for a 10 μm thick liquid crystal cell of optical density $D = 1$. Incident laser beam power $I_0 = 30$ mW; modulation frequencies $f = \omega/2\pi = 125$ Hz and 1250 Hz.

thermal capacity of the two materials), $\beta = 2.3 \times 10^5$ l/m is the absorption coefficient of the dye. The calculation procedure is described in [20,21]. The result is shown in Fig. 7 for a 10 μm thick cell (with optical density $D = 1$ in the isotropic phase) irradiated with laser beam of 30 mW power at two modulation frequencies, $f = \omega/2\pi = 125$ Hz and 1250 Hz.

Each curve shows a maximum (due to the dissipation of thermal energy in glasses) and well-pronounced asymmetry (due to the light absorption gradient). With increasing frequency, the increment ratio $\xi = \Delta T_r / \Delta T_f = \Delta T(z = d = 10 \mu$m$)/\Delta T(z = 0)$ decreases from 0.62 (125 Hz) to 0.44 (1250 Hz). It means that, at enhanced frequency, it would be easier to separate contributions to the pyroresponse from opposite interfaces. On the other hand, the absolute value of the increment also decreases and the measurements of the pyroelectric response become more difficult due to lower signal to noise ratio. Note that the calculated value $\xi = 0.62$ (125 Hz) is not too much different from the value 0.52 found experimentally at the same frequency, despite the roughness of the model (we have assumed uniform illumination in the cell plane, and neglected the absorption in the SnO₂ electrodes and multiple reflections of light). In further calculations we shall use $\xi = 0.52$ as the most reliable value.

IV. SURFACE AND FLEXOELECTRIC POLARIZATION

With the increment ratio known we can separate contributions to the total pyroelectric response from the two surfaces and the bulk of any cell (HH, PP, or HP). First, it should be done separately for the X and Y components and then the modulus of the response can easily be found (at this stage the background signal from the isotropic phase is subtracted). Then, integrating over temperature we find the surface and flexoelectric polarization of the nematic phase on an arbitrary scale; Finally, we apply a calibration procedure to find the absolute magnitudes of the polarizations.

A. Separation of different contributions to the total pyroelectric coefficient

For the X and Y components of the net nematic contribution (subscript N) to the total pyroelectric response, instead of set (7) we can write a new system of equations:

$$H_N(1-\xi)=a_{X,Y}(T) \quad \text{(homeotropic cell)}, \tag{11a}$$

$$P_N(1-\xi)=b_{X,Y}(T) \quad \text{(planar cell)}, \tag{11b}$$

$$P_N-\xi H_N+F=c_{X,Y}(T) \quad \text{(hybrid cell, illuminated from the planar side)}, \tag{11c}$$

$$\xi P_N-H_N+F=d_{X,Y}(T) \quad \text{(hybrid cell, illuminated from the homeotropic side)}. \tag{11d}$$

Here, the ratio $\xi=0.52$ is known; $F(T)$, $P_N(T)$, and $H_N(T)$ are temperature dependencies to be found [''nematic'' contributions to the total pyroresponse of the flexoelectric (bulk) and the solely planar and homeotropic surface polarizations]. Again the subscripts X and Y are omitted for $H, P,$ and F. Functions $a, b, c,$ and d are also known; they are the temperature dependent X or Y components of the total pyroresponse taken from Figs. 5 and 6 for HH, PP, and HP cells. Now the isotropic phase contribution is subtracted as a background. Moreover, a comparison is possible only for the same light energy absorbed; therefore, all four pyroresponse curves measured were reduced to the same absorbed energy, $A=1-T_{\text{opt}}=0.83$ (the average value for all the cells over the whole temperature range). After this procedure, instead of the response, we obtain a relative value of the *pyroelectric coefficient*, independent of absorption, and ready to be integrated to obtain the polarization.

At this stage, looking at Eqs. (11c) and (11d), we determine the signs of different contributions with respect to each other, taking as a reference the total pyroresponse of the hybrid cell, $c(T)$ or $d(T)$, and noting that all the temperature dependencies measured are qualitatively the same. We can conclude that, *in a hybrid cell, polarization P_{sp} and P_{sh} are parallel to P_{total}, but P_f is antiparallel with P_{total}.* The

vector sum of the X and Y components, that is, the modulus of the net pyroresponse corresponding separately to the flexoelectric polarization and solely planar and homeotropic surface polarizations (nematic parts), is shown in Fig. 8. They may also be considered as pyrocoefficients on an arbitrary scale. The curves for P and H are genuine curves corresponding to our measurements. Curve F shows nonmonotonic behavior, although physically senseless, but anticipated, because its X and Y components were obtained from Eq. (11c) as algebraic sums of the three curves with their maxima shifted along the temperature scale. The reason for the latter was discussed above.

After integrating all the curves presented in Fig. 8 over temperature we obtain the temperature dependencies of the surface and flexoelectric polarizations, still on the arbitrary scale (in mV K); see Fig. 9, left scale. At room temperature, the highest dependence is the surface polarization of the planar interface, the lowest is that of the homeotropic one. For the flexoelectric polarization the artificial feature mentioned becomes much less pronounced and, except for the phase transition region, the obtained data are quite reliable.

B. Absolute signs and magnitudes of the surface and flexoelectric polarizations

The absolute sign of the polarization of a homeotropic cell is known from our previous work [19] with pure 5CB,
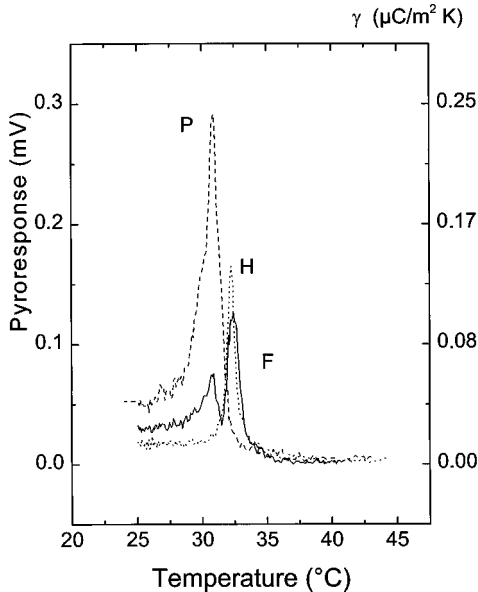
FIG. 8. Temperature dependence of the ''nematic'' pyrocoefficient corresponding separately to the flexoelectric polarization F and solely planar P and homeotropic H surface polarizations (without influence of the opposite interface). Left scale: pyroelectric response normalized to absorbed energy. Right axis: absolute scale for pyroelectric coefficient.
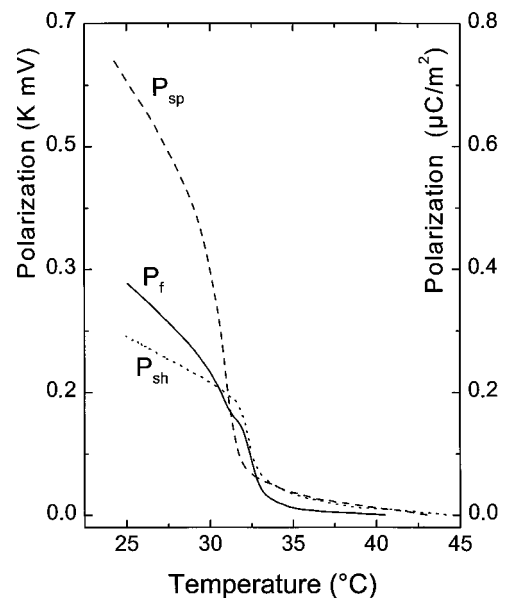
FIG. 9. Temperature dependencies of the surface (planar P_{sp}, homeotropic P_{sh}) and flexoelectric (P_f) polarizations. Left scale corresponds to the integral of pyroresponse shown in Fig. 8; right scale is absolute.

where we developed a calibration procedure that used the pyroelectric response to a $Nd^{3+}YAG$ laser pulse. In this case, there was no problem with phase shifts and the direction of the polarization could be found straightforwardly (it should be noted that, opposite to the present case, in [19] the illumination was performed through the grounded transparent electrode). Recently, we have repeated the same procedure with the dye-doped 5CB. The result is consistent with the previous measurements: *the surface polarization at the homeotropic interface is directed from the liquid crystal to the substrate.* Therefore with the results of Sec. IV A the genuine signs of all the contributions (for 5CB with 1% PcVO) are as follows:

(i) Surface (nematic) polarization at the *planar* SnO_2-polyimide interface is directed *toward* the liquid crystal.

(ii) Surface (nematic) polarization at the *homeotropic* SnO_2-polyimide interface is directed *outward* from the liquid crystal.

(iii) *Flexoelectric* polarization of a hybrid cell is directed *from the homeotropic to the planar interface (negative flexoelectric coefficient as in* [19]).

(iv) *Total* polarization of a hybrid cell *in this particular case* is determined mostly by the sum of the surface polarizations and directed *from the planar to the homeotropic interface.*

The absolute calibration of data presented in Figs. 8 and 9 has been done by their comparison with the pyroelectric response of a ferroelectric liquid crystal ZhK1005. The spontaneous polarization P_0 (and, consequently, the pyroelectric coefficient) of pure ZhK1005 is well known [22]. However, for the present work, a special mixture of ZhK1005 was prepared with the same concentration (1 wt. %) of PcVO. A standard (SSFLC) cell had the same thickness and absorbed the same amount of light energy at the laser wavelength $A = 1 - T_{opt} \approx 0.8$ as our nematic cells. The pyroelectric response of the ferroelectric cell is shown on the top of Fig. 10 (left scale). The bias voltage is necessary in order to orient all the ferroelectric domains with their P_0 vectors in one direction, along the field. The signal coming from the bulk spontaneous polarization is three orders of magnitude higher than that observed with nematic cells, and contributions from the surface polarizations may be neglected completely.

After integrating the pyroresponse over temperature, we obtain the temperature dependence of polarization shown in Fig. 10 (bottom). Independently, by the conventional repolarization current technique (with the same voltage ± 10 V), spontaneous polarization of the cell was measured; therefore, the absolute scale shown at the left axis was found (for example, the mixture has $P_0 = 70$ nC/cm^2 at 30 °C). After this, the correct scale (in $\mu C/m^2 K$) was introduced into Fig. 10 (top, right axis). Comparison of the left and right axes in Fig. 10 enables us to install the absolute scales into Fig. 8 and finally into Fig. 9 (right axes). Therefore the main result of the present paper is Fig. 9 with the right scale, just established.

V. DISCUSSION

As far as we know, the temperature dependencies of the nematic surface polarizations have been found for the first
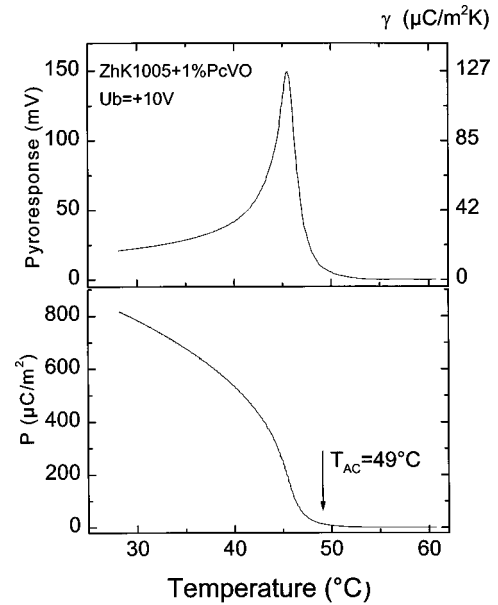

FIG. 10. Top: pyroelectric response of a ferroelectric cell filled with ZhK1005+1% PcVO mixture, bias voltage +10 V (left scale) and the corresponding pyroelectric coefficient (right scale). Bottom: polarization of the same cell found by integrating pyroresponse with subsequent fitting to the $P_0(T)$ known from independent measurements.

time. It is clear from Fig. 9 that the behavior of both the surface and flexoelectric polarizations correlates qualitatively with that of the orientational order parameter. We also know the absolute sign and magnitude of the polarizations and may compare them with what is anticipated from simple physical models.

Let us first discuss the surface polarization of the homeotropic interface. The polarization is directed from the bulk of 5CB into the surfactant covered SnO_2. In a molecule of 5CB, a longitudinal dipole moment (about 4 D) is mostly determined by the $-C \equiv N$ group and directed from a nitrogen to a carbon atom; that is, from the polar head to the hydrophobic tail of the molecule. The measured sign of the polarization corresponds to the orientation of 5CB molecules with their hydrophobic tail attached to the electrode. This result agrees with observations made by Forget *et al.* [23] and may be accounted for by the association of 5CB molecules in dimers. At 25 °C, the magnitude of the polarization averaged over the cell thickness 10 μm is $P_{sh} = 0.29$ $\mu C/m^2$. Usually the surface polarization is presented as a surface density of molecular dipoles and, in this case, its dimension coincides with that of the flexoelectric coefficient, $p_{sh} = P_{sh} d = 2.9$ pC/m or 8.7×10^{-5} cgs units (statV). This number may be compared with the maximum value corresponding to a monolayer of dipolar molecules with the perfect polar order, $p_{max} = N_m \mu = 67$ pC/m or 2×10^{-3} statV (here $N_m \approx 5 \times 10^{18}$ m^{-2} is the surface density of homeotropically oriented 5CB molecules with cross section 20 Å^2 and $\mu = 4$ D is the molecular dipole moment). Therefore the nematic part of the surface polarization is about 4% of the limiting value.

The sign of the surface polarization of a planar interface corresponds to P_{sp} directed from the interface to the bulk of 5CB and the magnitude of the polarization averaged over the cell thickness 10 μm is much higher than in the previous

case $P_{sp} = 0.73 \, \mu C/m^2$ (at 25 °C); therefore, $p_{sh} = 7.3 \, pC/m$ or $2.2 \times 10^{-4} \, statV$. 5CB molecules have no transverse dipole moment and such a polarization might only be provided by the ordoelectric term of the quadrupolar origin. It is known that the nematic order parameter at the polyimide interface significantly exceeds that in the bulk [24], and the ordoelectric polarization can be comparable with the flexoelectric one [2].

The bulk flexoelectric polarization is directed from the homeotropic to the planar boundary. At 25 °C the magnitude is equal to $P_f = 0.38 \, \mu C/m^2$. The corresponding sum of the flexoelectric coefficients $(e_1 + e_3) = 2dP_f = -8.4 \, pC/m$ $(-2.5 \times 10^{-4} \, statV)$ is close to the values reported earlier [14]; however, here the correct sign and the temperature dependence of the genuine flexoelectric polarization of 5CB is measured.

VI. CONCLUSION

In conclusion, using a pyroelectric effect based technique, the signs and absolute magnitude of the surface polarizations for a phthalocyanine dye doped 5CB at the planar and homeotropic interfaces have been found over the entire temperature range of the nematic phase; particularly, the ''nematic'' surface polarization at the polyimide-treated planar interface is directed toward the bulk (the magnitude at 25 °C is 7.3 pC/m), but at the surfactant treated homeotropic interface it is directed outward from the bulk (the magnitude at 25 °C is 2.9 pC/m). The sum of the flexoelectric coefficients $(e_1 + e_3) = -8.4 \, pC/m$ at 25 °C; the flexoelectric polarization in a hybrid cell is directed from the homeotropic to the planar interface. The temperature behavior of all the polarizations qualitatively correlates with that of the orientational order parameter.

[1] A. G. Petrov and A. Derzhanski, Mol. Cryst. Liq. Cryst. **41**, 41 (1977).

[2] G. Barbero, I. Dozov, J. F. Palierne, and G. Durand, Phys. Rev. Lett. **56**, 2056 (1986).

[3] R. B. Meyer, Phys. Rev. Lett. **22**, 918 (1969).

[4] J. Prost and J.-P. Marcerou, J. Phys. (Paris) **38**, 315 (1977).

[5] P. Guyot-Sionnest, H. Hsiung, and Y. R. Shen, Phys. Rev. Lett. **57**, 2963 (1986).

[6] Y. R. Shen, Nature (London) **337**, 519 (1989).

[7] V. G. Nazarenko, R. Klouda, and O. D. Lavrentovich, Phys. Rev. E **57**, R36 (1998).

[8] L. M. Blinov and V. G. Chigrinov, *Electro-optic Effects in Liquid Crystal Materials* (Springer-Verlag, New York, 1993).

[9] D. Schmidt, M. Schadt, and W. Helfrich, Z. Naturforsch. A **27**, 277 (1972).

[10] J. Prost and P. S. Pershan, J. Appl. Phys. **47**, 2298 (1976).

[11] A. Derzhanski, A. Pertrov, and M. Mitov, J. Phys. (Paris) **39**, 273 (1978).

[12] I. Dozov, Ph. Martinot-Lagarde, and G. Durand, J. Phys. (France) Lett. **43**, L365 (1982).

[13] B. Valenti, C. Bertoni, G. Barbero, P. Taverna-Valabrega, and R. Bartolino, Mol. Cryst. Liq. Cryst. **146**, 307 (1987).

[14] P. R. Maheswara Murthy, V. A. Raghunatan, and N. V. Madhusudana, Liq. Cryst. **14**, 483 (1993).

[15] S. R. Warrier and N. V. Madhusudana, J. Phys. II **7**, 1789 (1997).

[16] A. Petrov, in *Physical Properties of Liquid Crystals*, edited by D. Dunmur, A. Fukuda, and G. Luckhurst (EMIS Datareviews Series, 1999).

[17] L. M. Blinov, L. A. Beresnev, and W. Haase, Ferroelectrics **174**, 221 (1995).

[18] S. Palto, R. Barberi, M. Iovane, V. V. Lazarev, and L. M. Blinov, Mol. Mater. **11**, 277 (1999).

[19] L. M. Blinov, M. Ozaki, and K. Yoshino, Pis'ma Zh. Eksp. Teor. Fiz. **69**, 220 (1999) [JETP Lett. **69**, 220 (1999)].

[20] S. Bauer, J. Appl. Phys. **75**, 5306 (1994).

[21] A. Mandelis and M. M. Zver, J. Appl. Phys. **57**, 4421 (1985).

[22] L. M. Blinov, in *Modern Topics in Physics*, edited by A. Buka (World Scientific, Singapore, 1994), p. 337.

[23] S. Forget, I. Dozov, and Ph. Martinot-Lagarde, Mol. Cryst. Liq. Cryst. **329**, 605 (1999).

[24] H. Yokoyama, *Handbook of Liquid Crystal Research*, edited by P. Collings and J. Patel (Oxford University Press, New York, 1997), p. 179.